Investigation of Thermo-mechanical Behavior of Work Roll and Roll Life in Hot Strip Rolling

C. G. Sun*, C. S. Yun*, J. S. Chung* and S. M. Hwang**

(Received September 12, 1996)

Abstract

The effects of various process parameters on the detailed aspects of the thermo-mechanical behavior of work roll and on the roll life are investigated via a series of process simulation, using a mathematical model presented previously. The process conditions are discussed that are favorable or optimal in terms of reducing roll wear in the front finishing stands.

Key Words : Thermal-Mechanical, Roll Life, Roll Wear, Hot Strip Rolling

1. Introduction

In hot strip rolling, consumption of rolls contributes some 5~15 % of overall production costs,[1] and additional significant expenses are caused by interruptions of the production process for roll dressing, or shut-downs on account of the problems related to roll wear. As unprecedented considerations are being given to precision control of the product quality as well as to enhancing the production economy in most modern rolling practices, mill designers and shop engineers are keenly interested in reducing roll wear, either by optimizing the process conditions or by employing new roll materials.

The factors which can affect roll wear are diverse, as summarized in the references.[1~3] Among them, surface cracking induced by thermal fatigue and abrasion were accepted as the two main factors governing roll wear in hot strip rolling. In the past,

several investigators attempted to find a quantitative relationship between the thermo-mechanical behavior of the roll and roll wear, in order to reveal the process conditions favorable in terms of retarding roll wear. Most of these works were focused on the roughing and front finishing stands where roll wear is believed to be mainly due to thermal fatigue, as summarized below.

Williams and Boxall[2] determined the approximate value of the plastic strain amplitude of the circumferential, thermal stress-strain hysteresis loop suffered by a material point on the roll surface on each revolution, based on the predicted temperature distributions in the roll. The plastic strain amplitude was then used as a measure by which the roll life is evaluated, in conjunction with the low cycle fatigue life prediction model proposed by Coffin.[4] Stevens, Ivens, and Harper[5] also determined the plastic strain amplitude, based on the experimentally obtained temperature distributions

* Research Assistant
** Associate Professor in Department of Mechanical Engineering, Pohang University of Science and Technology (POSTECH), San 31, Hyoja Dong, Nam-Gu, Pohang 790-784, Korea

in the roll, and showed that the location of the water spray zone for roll cooling that led to the minimum plastic strain amplitude and therefore was optimal in the light of the roll life was on the delivery side, right after the roll exit. Sekimoto et al.[6] used the heat penetration depth and the maximum roll surface temperature as the measures by which the roll life is evaluated and derived the same conclusion regarding the optimal location of the spray zone. In particular, they calculated the depth of the surface crack, assuming that there exists a critical temperature below which crack generation is not possible. Ryu et al.[7] defined the thermal fatigue damage parameter as a function of the plastic strain amplitude and the number of revolution and showed that the parameter can be effectively used as a measure of evaluating the severity of roll wear.

The conclusions and implications regarding roll

wear derived from the above mentioned works were valuable resources to achieve better process control toward retarding roll wear. However, many simplifying assumptions had to be made during the development of the mathematical models for the prediction of the thermo-mechanical behavior of the roll, for example, simplified versions of the energy equation as well as of the stress-strain relation, the elementary rolling theory to calculate heat generation due to plastic deformation and interface friction, and neglect of the effect of mechanical loading, so forth. Consequently, those works could address only a portion of the diverse process parameters that may possibly influence roll wear significantly, and the predicted effect on the thermo-mechanical behavior was at best approximate. Thus, it was felt necessary to investigate the problem of roll wear on the basis of a more rigorous model, such as one presented in paper.[8] In this paper, the effect of roll material, roll speed, heat transfer coefficients, mill stand, friction, location of water spray zone for roll cooling, and cooling water temperature, was investigated via a series of process simulation on the detailed aspects of the thermo-mechanical behavior of the work roll and of its effect on roll wear. The process conditions were discussed that were favorable or optimal in terms of reducing roll wear in the front finishing stands.

Table 1 Process conditions used in simulation

Simulation Case No.	D_o (mm)	h_{lub} ($kW/m^2°C$)	H_o (mm)	Redu. (%)	Spray zone	V (mpm)	T_o (°C)	h_{wl} ($W/mm^2°$)	Roll material
1 (F_1)	810	60	34.46	48.6	A	75	1077	0.035	HSS
2 (F_1)	810	60	34.46	48.6	A	75	1077	0.035	Hi-Cr
3 (F_1)	810	60	34.46	48.6	A	75	1077	0.035	S.G.cast iron
4 (F_1)	810	60	34.46	48.6	A	25	1077	0.035	S.G.cast iron
5 (F_1)	810	60	34.46	48.6	A	150	1077	0.035	S.G.cast iron
6 (F_1)	810	60	34.46	48.6	A	75	1077	0.0035	S.G.cast iron
7 (F_1)	810	60	34.46	48.6	A	75	1077	0.35	S.G.cast iron
8 (F_1)	810	40	34.77	43.3	B	70	1040	0.035	S.G.cast iron
9 (F_1)	810	60	34.77	43.3	B	70	1040	0.035	S.G.cast iron
10* (F_1)	810	60	34.46	48.6	B	75	1077	0.035	S.G.cast iron
11 (F_1)	810	60	34.46	48.6	B	75	1077	0.035	S.G.cast iron
12* (F_1)	810	60	34.46	48.6	B	75	1077	0.035	S.G.cast iron
13 (F_2)	810	60	17.72	39.2	B	124	1030	0.035	S.G.cast iron
14 (F_3)	810	60	10.78	37.9	B	200	1011	0.035	S.G.cast iron
15 (F_1)	810	60	34.77	43.3	C	70	1040	0.035	S.G.cast iron
16 (F_1)	810	60	34.77	43.3	D	70	1040	0.035	S.G.cast iron
17 (F_1)	810	60	34.77	43.3	E	70	1040	0.035	S.G.cast iron
18 (F_1)	810	60	34.77	43.3	F	70	1040	0.035	S.G.cast iron

Note : 1. D_o : Roll diameter, diameter of core is 650mm.

2. V : Roll speed, T_o : Entry temperature of strip, H_o : Entry thickness of strip.

3. In case 10, friction coefficient $\mu = 0.25$, in case 12, $\mu = 0.35$; in other cases, $\mu = 0.3$.

4. h_{wl} : Heat transfer coefficient directly under the spray.

5. Strip material is JS-SS400.

6. The carbon content of JS-SS400 is 0.155%, the width of JS-SS400 strip is 1524 mm.

Table 2 The thermal and mechanical properties of strips

Material	Flow stress	K		ρc		ρ
		Temp. (°C)	($W/mm \cdot °C$)	Temp. (°C)	($J/mm^3 \cdot °C$)	(kg/m^3)
JS-SS400	from Shida	0	0.0519	50-100	0.00382	7860
		100	0.0511	150-200	0.00408	
		200	0.0490	250-300	0.00418	
		300	0.0461	300-350	0.00438	
		400	0.0427	350-400	0.00451	
		500	0.0394	450-500	0.00520	
		600	0.0356	550-600	0.00589	
		700	0.0318	650-700	0.00665	
		800	0.0260	700-750	0.01126	
		1000	0.0297	750-800	0.00747	

Note : 1. K : Thermal conductivity, ρc : Specific heat capacity, ρ : Density.

• Preliminaries

Investigation was focused on the front ones (F_1, F_2, F_3) of the seven finishing stands in POSCO No. 2 hot strip mill. The strip materials considered was JS-SS400, a plain carbon steel with 0.155 percent carbon. The flow stress expression for the carbon steel derived by Shida[9] were used. For the work roll, Hi-Cr roll, HSS roll, and S. G. cast iron roll were considered. Process conditions, thermal and mechanical properties of the strips, thermal and mechanical properties of the rolls, and the information regarding the roll cooling are listed in Tables 1~5.

The predicted temperature profile along the surface of the work roll is illustrated in Fig. 1(a). The area showing the abrupt variation in the surface temperature was the bite region, while the areas showing the minimum surface temperature repre-

Table 4 The mechanical properties of rolls

Material		α		ρ	E	ν
		Temp. (°C)	($10^{-6}/K$)	(kg/m^3)	(kN/mm^2)	
HSS	Shell	82	7.63	7620	220	0.287
		199	11.0			
		294	10.9			
		383	11.8			
		447	12.1			
		492	12.6			
		506	12.7			
	Core	20-100	11.5	7100	160	0.275
		20-200	11.8-12.6			
		20-300	12.6			
		20-400	13.2			
		20-500	13.4			
		20-600	13.5			
		20-700	13.8			
Hi-Cr	Shell		13.0	7600	220	0.3
	Core		12.0	7200	205	0.3
S.G. cast iron			12.5	7100	173.2	0.275

Note :

1. α : Coefficient of linear thermal expansion, ρ : Density.

2. E : Young's modulus, ν : Poisson's ratio.

3. The compressive yield stress of Hi-Cr roll is 1600 - 1650 MPa at 20 °C.

4. The tensile strength of HSS roll is 1000 MPa at 20 °C and 600 MPa at 500 °C.

Table 3 The thermal properties of rolls

Material		K		ρc	
		Temp. (°C)	($W/mm \cdot$ °C)	Temp. (°C)	($J/mm^3 \cdot$ °C)
HSS	Shell	110	0.0224	500	0.004572
		120	0.0230		
		205	0.0246		
		213	0.0249		
		254	0.0254		
		316	0.0262		
		398	0.0264		
		412	0.0269		
		502	0.0272		
		522	0.0273		
	Core	20-500	0.036	20-200	0.0032731
				20-300	0.0035074
				20-400	0.0035997
				20-500	0.0036565
				20-600	0.0038065
				20-700	0.0042813
Hi-Cr	Shell		0.02		0.004484
	Core		0.027		0.004248
S.G. cast iron		100	0.04354	20-200	0.0032731
		200	0.04312	20-300	0.0035074
		300	0.04019	20-400	0.0035997
		400	0.03768	20-500	0.0036565
		500	0.03517	20-600	0.0038065
				20-700	0.0042813

Note : K : Thermal conductivity, ρc : Specific heat capacity.

Table 5 The characteristics of roll cooling

Cooling style	Entry-side Cooling range (°)	Exit-side Cooling range (°)	Entry-side T_{w1} (°)	Exit-side T_{w2} (°)	
A	110-230	230-250	20	20	
B	79-103	258-296	20	20	see Fig.10 (a)
C		278-340		20	see Fig.10 (b)
D		278-340		0	see Fig.10 (b)
E	30-54	302-340	20	20	see Fig.10 (c)
F	30-54	302-340	20	0	see Fig.10 (c)

Note : 1. directly under the spray : $h_{w1} = 0.035$ ($W/mm^2°C$).

2. in the other region : $h_{w2} = 0.00875$ ($W/mm^2°C$).

3. T_{w1}, T_{w2} : cooling water temperature.
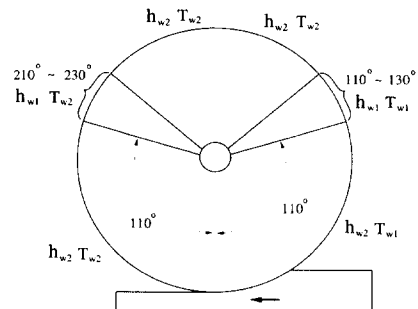
A
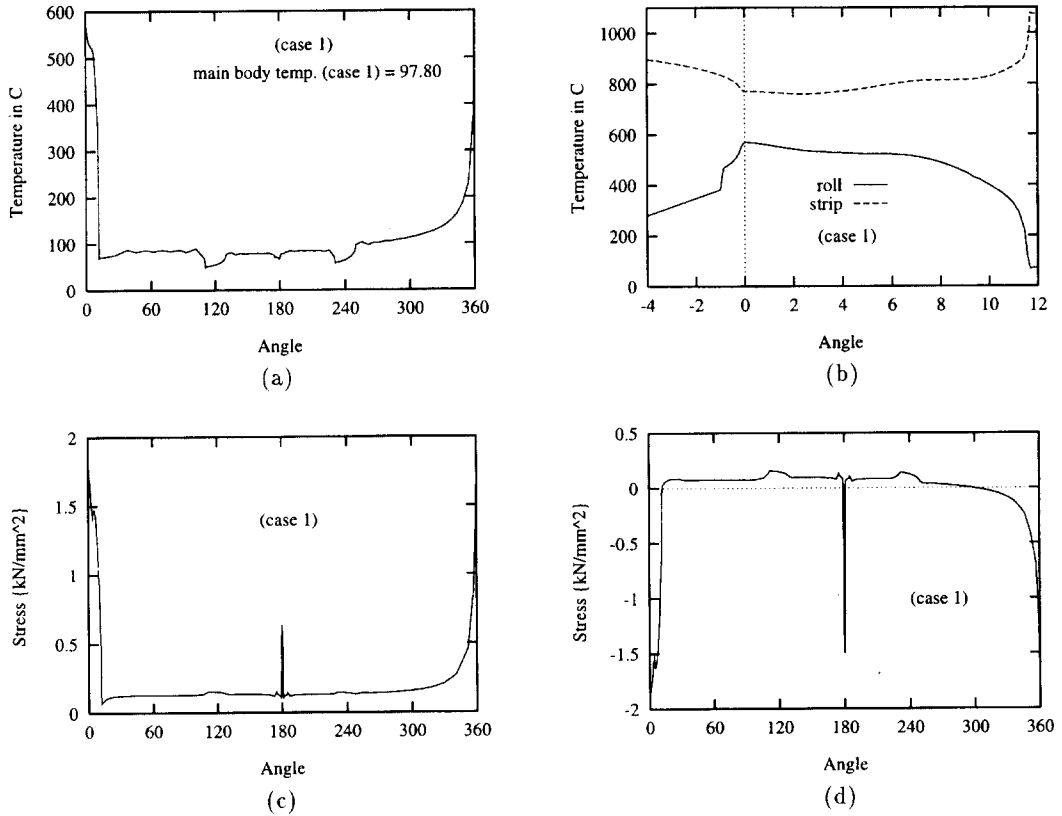
Fig. 1 (a) Temperature distributions along the surface of the work roll (b) Roll and strip surface temperatures at the bite region (c) Effective stress distributions along the surface of the roll (d) $\sigma_{\theta\theta}$ distributions along the surface of the roll

sent the zones where the water is sprayed to cool the roll. As may be expected, the maximum roll surface temperature occurred at the roll exit, as shown in Fig. 1(b).

Fig. 1(c) shows the values of the effective stress that a material point on the surface of the work roll experiences on each revolution. As far as the circumferential stress is concerned, the maximum compressive stress occurs at the bite region and at the backup roll-work roll interface, and the maximum tensile stress occurs at the water spray zone, as shown in Fig. 1(d). Note that the magnitude of the maximum circumferential stress at the bite region as well as at the water spray zone were very close to that of the effective stress at the same region. In these regions the radial stresses were

much smaller than the circumferential stress, and the axial stress was almost the same as the circumferential stress.

Fig. 2 shows that approximately, ninety percent of the magnitude of the compressive circumferential stress at the bite region was due to thermal loading and the rest due to mechanical loading. On the other hand, the magnitude of the compressive circumferential stress at the backup roll-work roll interface due to mechanical loading was reduced by the presence of thermal loading, about seven percent.

In this investigation, the circumferential stress distributions were predicted based on the purely elastic behavior of the material. However, compared to the compressive yield strength of the roll
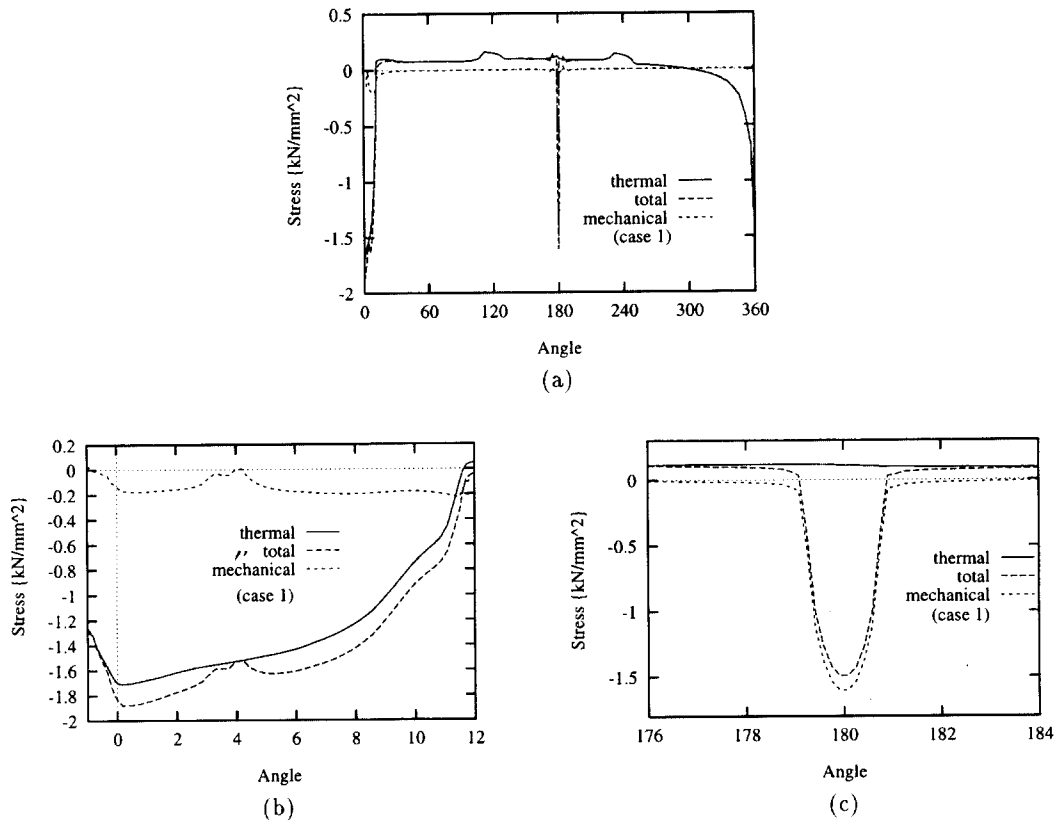
Fig. 2 (a) $\sigma_{\theta\theta}$ along the surface of the roll (b) $\sigma_{\theta\theta}$ along the surface of the roll at the bite region
(c) $\sigma_{\theta\theta}$ along the surface of the roll at the region contacting with the back-up roll

materials, the effective stress at the bite region is large enough to ensure the occurrence of the plastic deformation of the material point when it passes the bite region. As a result, the actual magnitude of the maximum tensile circumferential stress can be much larger than the predicted value, depending on the amount of the compressive, plastic circumferential strain suffered by the material point. Thus, after the material point leaves the bite region, it may be fractured due to the large tensile stress. Or it may deform plastically again, forming a hysteresis loop. To evaluate the roll life, it was assumed that roll wear is caused by the thermo-mechanical, low cycle fatigue of the material point as it follows the hysteresis loop, based on the theories of Williams and Boxall[2] and Parke and Baker.[10]

The approximate shape of the hysteresis loop and the plastic strain amplitude can be derived from the predicted elastic circumferential stress and strain distributions, provided the information regarding the yield stress of the roll material is given, as follows : First, we plot all the data points representing the elastic circumferential stress-elastic circumferential strain values that a material point on the roll surface exhibits on each revolution, as shown in Fig. 3 (a). As can be seen in Fig. 1, the maximum values of the compressive circumferential stress and strain, denoted by $\sigma_{\theta\theta}^{C}$ max and ε_{2} in the figure, occurred near the roll exit, while the maximum tensile stress and strain, denoted by $\sigma_{\theta\theta}^{T}$ max and ε_{1}, occurred at the water

(a)

(b)
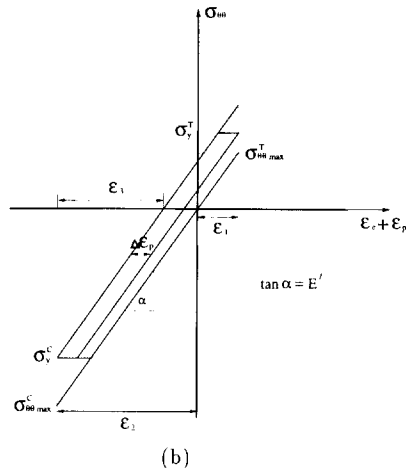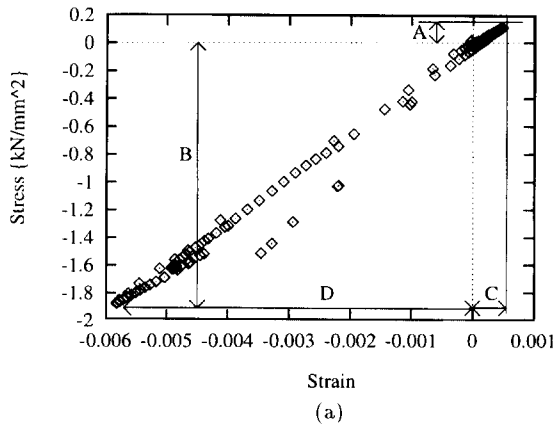
Fig. 3 (a) **Elastic stress** $(\sigma_{\theta\theta})$ **vs elastic strain** $(\varepsilon^e = \varepsilon_{\theta\theta} - \alpha\Delta T)$
curve, $(A: \sigma_{\theta\theta}^T{}_{max}, \ B: \sigma_{\theta\theta}^C{}_{max}, \ C: \varepsilon_1, \ D: \varepsilon_2),$
(b) hysteresis loop

spray zone where the temperature is minimum. Considering that the effective stress level is not sufficiently high for the plastic deformation to occur at the back-up roll – work roll interface, a few scattered data points which represent the compressive circumferential stress-strain values that a material point on the roll surface exhibits as it passes the back-up roll – work roll interface can be neglected, since they will not affect the plastic strain amplitude. Then, the trajectory that the material point follows on each revolution provided that the material is elastic, or the elastic circumferential stress-

strain loop, is approximated by a straight line with slope E', or

$$\sigma_{\theta\theta} = E' \varepsilon^e \qquad (1)$$

The approximate hysteresis loop, shown in Fig. 3(b), was constructed from the predicted elastic stress-strain loop, under the following assumptions : (1) the circumferential stress is equal to the yield stress in magnitude during plastic deformation, and (2) the maximum circumferential strains ε_1 and ε_2 are unaltered by the occurrence of the plastic deformation. The plastic strain amplitude of the hysteresis loop thus obtained can be expressed by

$$\Delta\varepsilon_p = \frac{1}{E'}(\sigma_{\theta\theta}^C max + \sigma_{\theta\theta}^T max - \sigma_y^C - \sigma_y^T) \qquad (2)$$

where σ_y^C and σ_y^T are the compressive yield strength at the temperature at which the maximum compressive circumferential stress occurs, and the tensile yield strength at the room temperature, respectively. Their values for S. G. cast iron rolls are given by [5] :

$$\sigma_y^C = 2.3499 - 0.003456 \cdot T \ (kN/mm^2) \qquad (3)$$

$$(T \ is \ in \ °C)$$

$$\sigma_y^T = 0.2405 \ (kN/mm^2) \qquad (4)$$

The plastic strain amplitude thus obtained was used as a measure to evaluate the roll life, in conjunction with the low cycle fatigue life prediction model proposed by Coffin [4]

$$\Delta\varepsilon_p \sqrt{N} = A = \text{Constant} \qquad (5)$$

For a cast iron material, Baron and Bloomfield [11] determined by experiment that A=0.06 corresponded to the number of cycle N to produce the crack of 0.5 mm deep from the surface, which was selected for this investigation. It should be noted

that, due to the fact that the loading conditions as well as the roll material are different from those used in their experiments, the number of cycle N thus predicted does not necessarily represent that required to achieve the same crack depth. However, it may be used to estimate the percent of the life of the work roll to be increased (or decreased) by altering the process conditions.

• Effect of roll material

Fig. 4(a) shows that among the three roll materials, the cast iron roll resulted in the greatest minimum strip surface temperature and the smallest maximum roll surface temperature, or the greatest amount of heat flux from the strip to the roll. Heat flux associated with HSS roll was the second great-

est, indicating that the heat flux was increased with the increasing thermal conductivity of the roll material. Comparing HSS roll with Hi-Cr roll, HSS roll led to the smaller maximum compressive circumferential stress as well as the smaller maximum roll surface temperature, as shown in Fig. 4(b), while the maximum tensile circumferential stress was similar to that obtained when Hi-Cr roll was used. It is evident from equation[2] that the smaller roll surface temperature combined with the smaller maximum compressive circumferential stress would result in the smaller plastic strain amplitude as well as the greater hardness of the roll material, indicating that a much longer service life associated with the HSS roll than with the Hi-Cr roll is not only due to the high yield strength of the
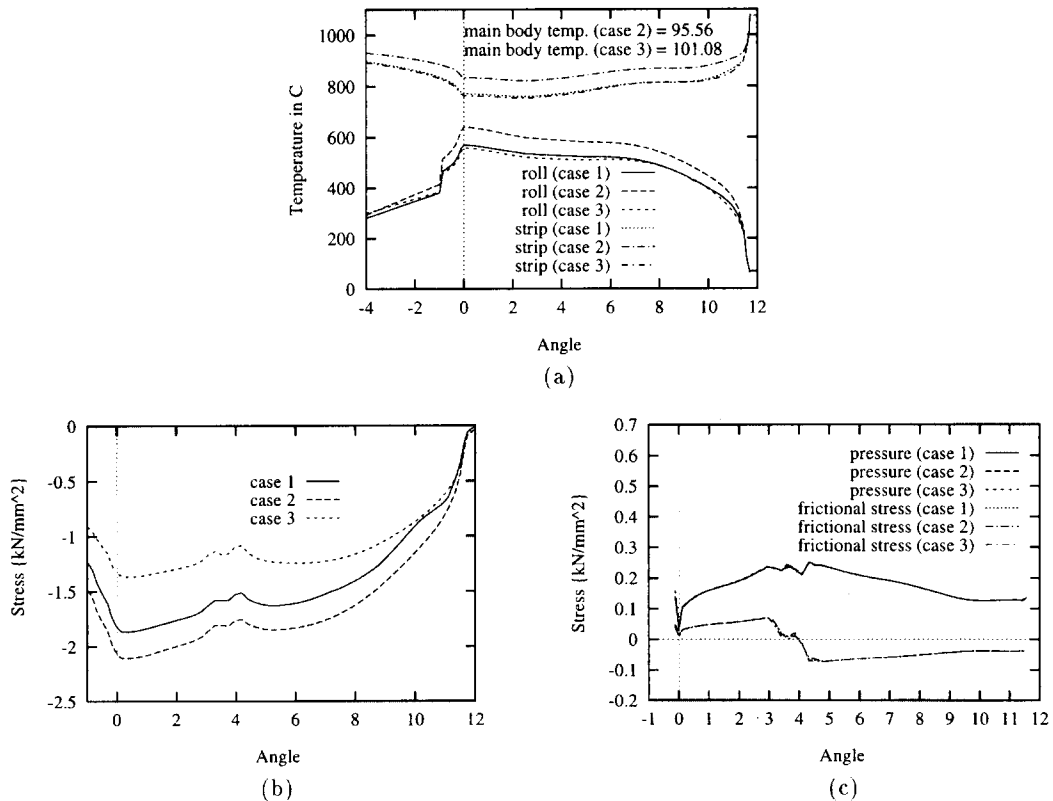
Fig. 4 (a) Roll and strip surface temperatures at the bite region
(b) $\sigma_{\theta\theta}$ distributions along the surface of work rolls at the bite region
(c) Roll pressure and frictional stress distributions along the surface of work rolls at the bite region

material but partly due to the fact that its thermo-mechanical behavior is more favorable in terms of reducing roll wear. The roll pressure and the frictional stress distributions at the bite region were found to be insensitive to the roll material, as shown in Fig. 4(c).

• Effect of roll speed

Fig. 5(a) shows that the minimum roll surface temperature at the cooling region and the main body temperature of the roll were increased with the increasing roll speed. At the bite region, the maximum roll surface temperature was decreased with the increasing roll speed, due to the decrease in the contact time, when the roll speed is relative-

(a)

(b)

Fig. 5 (a) Effect of roll speed on roll surface temperature roll main body temperature and strip surface temperature
(b) Effect of roll speed on $\sigma_{\theta\theta}$, roll force and roll life

ly low. However, when the roll speed exceeded a certain value, or the critical speed, the tendency was reversed, with the maximum roll surface temperature being increased with the increasing roll speed, as the increasing heat flux from the strip as well as the increasing heat generated by friction overcame the effect of the decrease in the contact time. As may be seen from the figure, the critical speed resided between 75 mpm and 150 mpm, for rolling at F_1 under the given process conditions. The effect of roll speed on the minimum strip surface temperature was also shown in the figure, which was found to be much more pronounced than the effect on the roll surface temperature.

Contrary to the negligible effect of roll speed on the roll surface temperature at the bite region, it significantly affected the circumferential stress at the bite region. The maximum compressive circumferential stress was significantly decreased and the maximum tensile circumferential stress was slightly increased as the roll speed was increased, due to the increase in the temperature of the main body of the roll with the increasing roll speed, as shown in Fig. 5(b). The result was the increase of the roll life with the increasing roll speed. It was noted that the effect was more drastic at a smaller interface heat transfer coefficient.

As the roll speed is increased, both the temperature and the strain rate of the strip material are increased, and the flow stress may increase or decrease, depending on which variable has a greater effect. At F_1, it was the strain rate that had more influence on the flow stress, and consequently, the roll pressure and the roll force were increased with increasing roll speed, as shown in Fig. 5(b). Considering that the increase in the roll pressure accelerates roll wear due to abrasion, it is evident that there exists an optimal roll speed in terms of overall roll wear due to fatigue and abrasion. It is not possible to determine the optimal roll speed, since a quantitative model which relates the thermo-mechanical behavior to overall roll wear
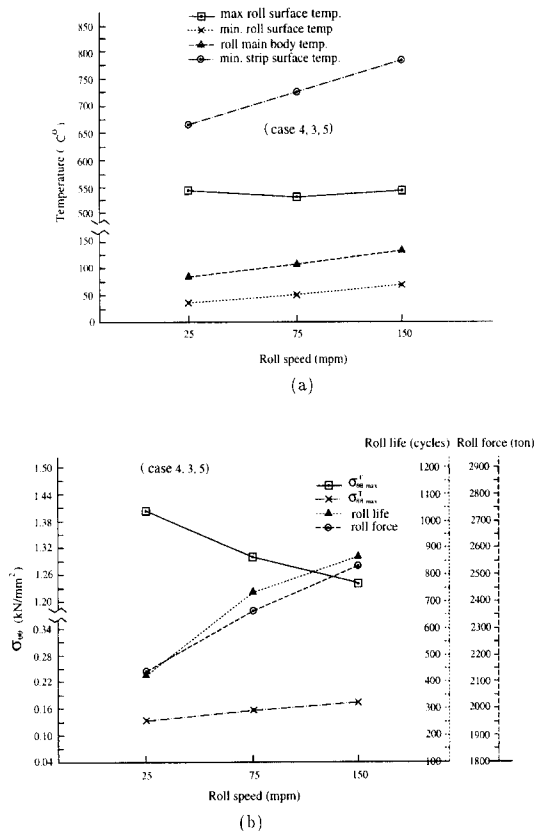
due to both fatigue and abrasion is currently not available. However, the optimal speed must at least be greater than the critical speed, because in the speed range below the critical speed, the effect of the decrease in the roll surface temperature at the bite region with the increasing roll speed would result in the increase in the hardness of the roll material, compensating the effect of the increase in the roll pressure. The critical speed may vary from stand to stand and also may depend on the pass schedule.

• Effect of heat transfer coefficient at water spray zone

One of the problems regarding roll cooling is to ascertain just what particular values of cooling water pressure and water flow rate to be applied to the roll are beneficial in terms of the roll life, as noted by Harper.[3] As an attempt to answer this aspect of the problem, at least qualitatively, investigated was the effect of the heat transfer coefficient at the spray zone between the roll and the water flux, since it must be related to the flow rate such that it increases with the increasing flow rate, as may be inferred from the empirical correlation relating the heat transfer coefficient at the descaling water spray zone between the strip and the water flux, derived by Sasaki et al.[12] Among the three values of the heat transfer coefficient tested, $h = 0.035 \ W/mm^{2\circ}C$ was believed to be closest to the actual values in the mill in most cases, as the measurements made by Poplawski and Seccombe[13] and also by Sekimoto et al.[6] resulted in 0.035 and 0.014 $W/mm^{2\circ}C$, respectively.

As was expected, both the roll surface temperature and the main body temperature were increased with the decreasing heat transfer coefficient. The effect was most clear at the cooling zone, while the strip surface temperature as well as the roll surface temperature at the bite region were less affected, as shown in Fig. 6(a). The maximum compressive circumferential stress as well as the
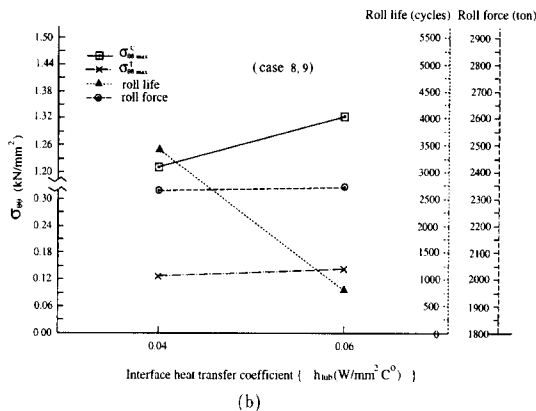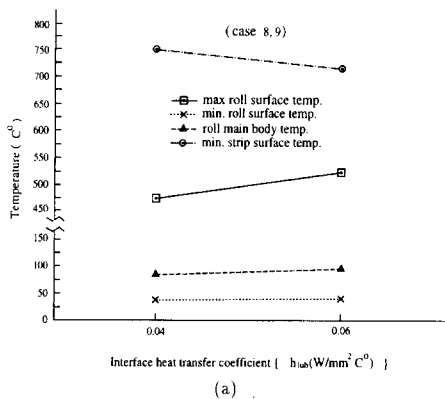

(a)

(b)
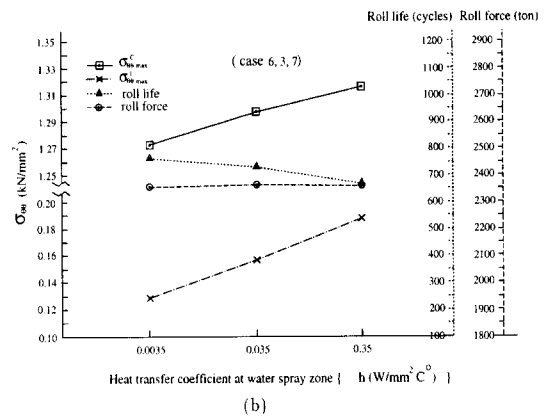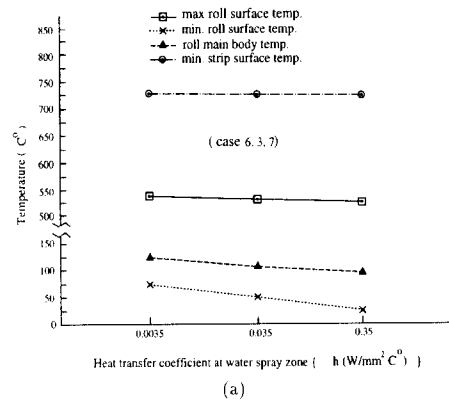
Fig. 6 (a) Effect of heat transfer coefficient at water spray zone on roll surface temperature, roll main body temperature and strip surface temperature
(b) Effect of heat transfer coefficient at water spray zone on $\sigma_{\theta\theta}$, roll force and roll life

maximum tensile circumferential stress were decreased with the decreasing heat transfer coefficient, resulting in the increase of the roll life with the decreasing heat transfer coefficient, as shown in Fig. 6(b). However, the increase in the roll life obtained by reducing the heat transfer coefficient seemed minor, considering the extremely wide range of the values of the heat transfer coefficient tested. This is due to the fact that the decrease of the heat transfer coefficient also resulted in the decrease in the yield strength of the material point passing the bite region, due to the increase in the roll surface temperature. From the result and also considering that roll wear due to abrasion would

increase as the heat transfer coefficient was reduced since the roll surface temperature was increased and the roll force remained unaffected. it may be deduced that while it is obvious that an excessive flow rate is detrimental, it is difficult to retard roll wear by reducing the flow rate.

• Effect of heat transfer coefficient at roll-strip interface

As seen in Fig. 7(a), the roll surface temperature as well as the main body temperature were decreased with the decreasing heat transfer coefficient. It is seen that the maximum roll surface temperature as well as the minimum strip surface

(a)

(b)

Fig. 7 (a) Effect of interface heat transfer coefficient on roll surface temperature, roll main body tem perature and strip surface temperature, (b) Effect of interface heat transfer coefficient on $\sigma_{\theta\theta}$, roll force and roll life

temperature were significantly affected. while the effect on the minimum roll surface temperature seemed relatively minor.

Fig. 7(b) shows that reducing the interface heat transfer coefficient can effectively lower the circumferential stress level. especially the maximum compressive circumferential stress. This was due to the fact that the rate of the decrease of the roll surface temperature at the bite region was much larger than that of the roll main body temperature. The resulting change in the roll life was so great as to make the interface heat transfer coefficient the single most important process parameter affecting the roll life while the effect of all the other process parameters are secondary. Considering that the effect of interface heat transfer coefficient on the roll force was negligible. it is evident that the decrease in the interface heat transfer coefficient is also effective in reducing the roll wear due to abrasion. According to Murata et al.,[14] the interface heat transfer coefficient may vary widely $(0.0058 - 0.4 \ W/mm^{2°}C)$, depending upon the type of the lubricant. The present results indicate that it is extremely important to select or to develop a proper lubricant which would exhibit as small an interface heat transfer coefficient as possible during rolling.

• Effect of friction

The effect of friction was such that about $25\,^{\circ}C$ increase in the maximum roll surface temperature resulted from 0.1 increase in the Coulomb friction coefficient in F_1 stand. as shown in Fig. 8(a). It was found that the roll main body temperature, the minimum roll surface temperature. the minimum strip surface temperature were little affected by the coefficient of friction.

Both the maximum compressive circumferential stress and the maximum tensile circumferential stress were increased with the increasing coefficient of friction. resulting in the decrease in the roll life, as shown in Fig. 8(b). The roll pressure as well as
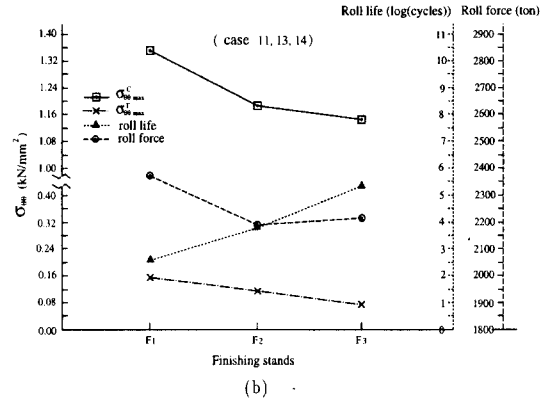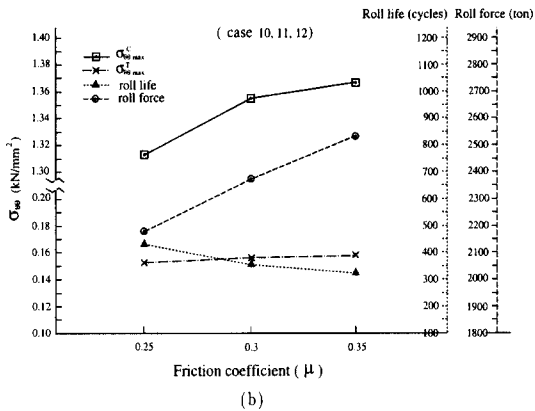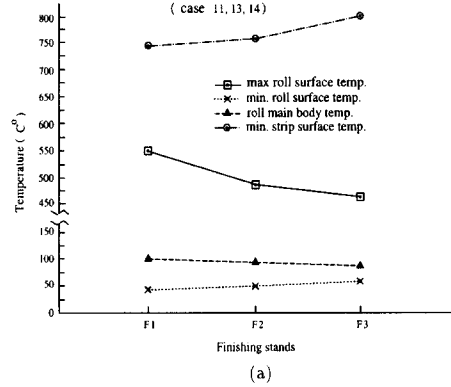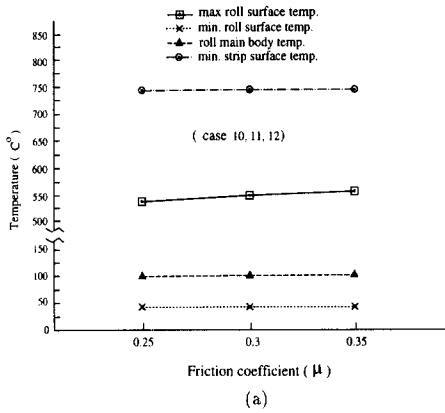
Fig. 8 (a) Effect of friction coefficient on roll surface
temperature, roll main body temperature and strip
surface temperature
(b) Effect of friction coefficient on $\sigma_{\theta\theta}$, roll force
and roll life

Fig. 9 (a) Effect of mill stand on roll surface temperature,
roll main body temperature and strip surface
temperature
(b) Effect of mill stand on $\sigma_{\theta\theta}$, roll force and roll life

roll force were also increased, with the rate of increase in the roll force being about 16 percent / 0.1 increase in the coefficient of friction. It was evident from these results that the coefficient of friction should be minimized in order to retard the roll wear, as other investigators, for example, Sekimoto et al.,[6] suggested.

• Effect of mill stand

The maximum roll surface temperature was decreased while the minimum strip surface temperature was increased as rolling was progressed from F_1 to F_3 stand, as shown in Fig. 9(a). This was due to the decrease in the time of contact between a

material point on the roll surface and the strip on each revolution, as confirmed by Stevens et al.,[5] Fig. 9(b) shows that the maximum compressive circumferential stress as well as the maximum tensile stress were reduced as rolling was progressed, resulting in the significant increase in the roll life in F_2 and further increase in F_3, compared to F_1 stand.

Examination of the surfaces of the used rolls before redressing in the POSCO hot strip mill[7] revealed that roll wear was most severe in F_2, while the severity of roll wear in F_1 and in F_3 appeared to be similar. Two theories may be conceived to explain the discrepancy between the pre-

dictions and observations. One is due to Williams and Boxall,[2] that severe roll wear observed in F_2 is caused by abrasion by hard iron oxides such as haematite and magnetite that were formed on the strip surface after the strip left F_1. The other is due to Stevens et al.,[5] that the interface heat transfer coefficient varies with the contact time. The latter seemed highly plausible, considering the remarkable effect of the interface heat transfer coefficient on the roll life, as revealed by the earlier investigation. Whatever the reasons for severe roll wear in F_2 are, it is evident that precise predictions of the effect of the mill stand require further research.

- ### • Optimization of location of water spray zone and cooling water temperature

One of the problem regarding roll cooling is to determine the location, or all the locations if two or more water spray zones exist, which is optimal in terms of the roll life. Also, optimization of the temperature of the cooling water may be important, if the roll life is significantly affected by it. The mathematical formulation of the present optimization problem can be given as follows :

Find the set of design variables, which are the location of the water spray zones Zwi and the corresponding cooling water temperatures Twi, i=1 , 2, ...n, that minimizes $\Delta \varepsilon_p$, which is defined by equation, under the given process conditions and following constraints

$$30° < Zwi < 160° \quad \text{for entry side spray}$$
$$200° < Zwi < 340° \quad \text{for delivery side spray} \quad (6)$$
$$T_{max} \leq \bar{T}_{max} \quad (7)$$

where, T_{max} is the maximum roll surface temperature and $\bar{T}_{max}$ is the maximum allowed temperature.

The two sets of the minimum and the maximum angles between which the water spray zones were supposed to reside, defined in equation,[6] were

(a)

(b)

(c)
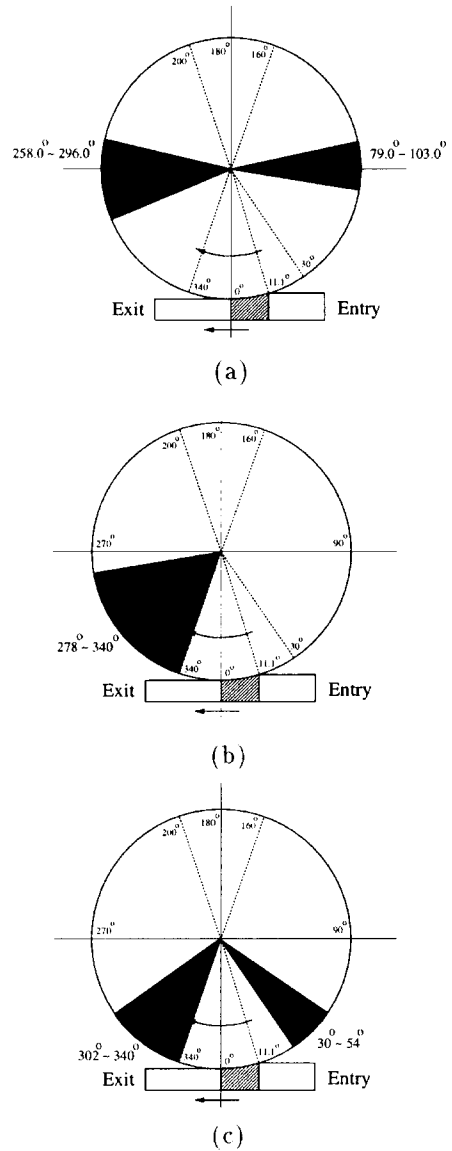
Fig. 10 (a) POSCO cooling design
(b) Optimum cooling zone (one spray)
**(c) Optimum cooling zones (two sprays)**

selected in order to avoid for the spray zones to overlap with the backup roll-work roll interface or with the bite region. Equation[7] was imposed in order for the optimal design to result in at least the same degree of roll wear due to abrasion as the conventional design.
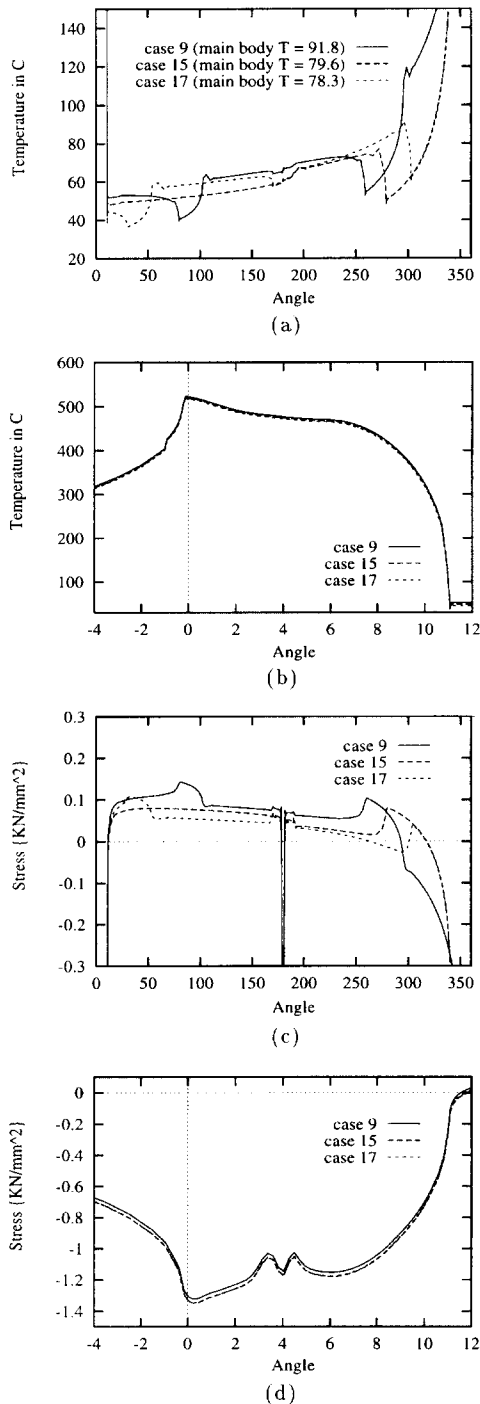
Fig. 11 (a) Temperature distributions along the roll surface
(b) Temperature distributions along the roll surface at the bite region
(c) $\sigma_{\theta\theta}$ distributions along the roll surface
(d) $\sigma_{\theta\theta}$ distributions along the roll surface at the bite region

As shown in Fig. 10(a), two water spray zones, one in the entry side (zone angle=24.0°) and one in the delivery side (zone angle=38.0°) of the roll, were used in POSCO hot strip mill. It was attempted to find the locations of these spray zones that would bring better results in terms of the roll life. Also attempted was to find the location of the water spray zone when only one spray (zone angle=62°) was used. The F_1 stand was selected for the investigation. $\overline{T}_{max} = 520.0°C$ was selected, considering that it was the maximum roll surface temperature resulting from the POSCO cooling design. The process conditions under which optimization was conducted were summarized as cases 15, 17 in Table 1. The cooling water temperature was assumed to be Tw = 20.0°C. To solve the above optimization problem, the present analysis model was combined with an optimization technique known as the Genetic Algorithm.[16,17] A genetic algorithm mimics the natural selection process by which a superior creature evolves while inferior ones fade out from their population as generations go on. The details of the genetic algorithm used for the present investigation was given in the reference .[18] Starting from the initial generation that consisted of four, arbitrarily chosen, sets of the design variables, optimization required approximately 50 to 150 generations before convergence.

For the case of one spray zone, its optimal location was at the roll exit, as shown in Fig. 10(b). The present result agreed with predictions made by Stevens et al.,[5] Parke and Baker,[10] and Sekimoto et al.,[6] For the case of two spray zones, the optimal locations were, one at the roll exit and the other at the roll entry, as shown in Fig. 10(c). As may be seen from Fig. 11, the optimal designs, compared to the POSCO design, resulted in the increase in the minimum roll surface temperature while the maximum roll surface temperature was little affected. The maximum compressive circumferential stress was greater than that resulting from the POSCO design, due to the decrease in the
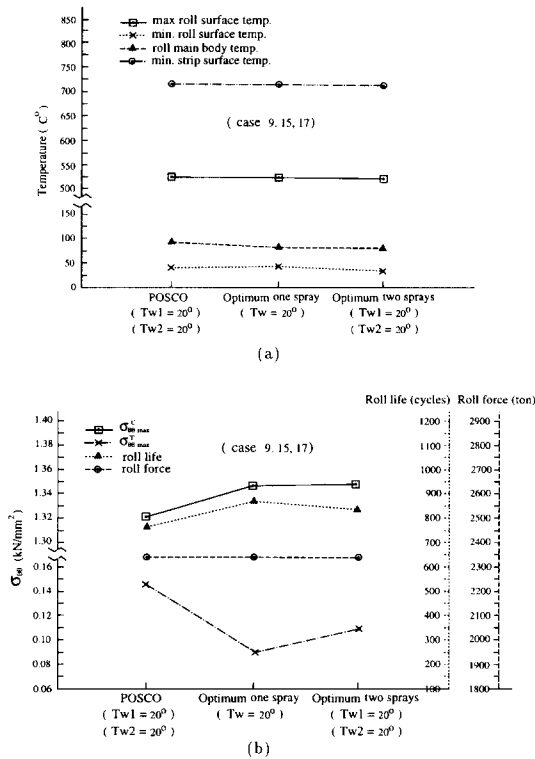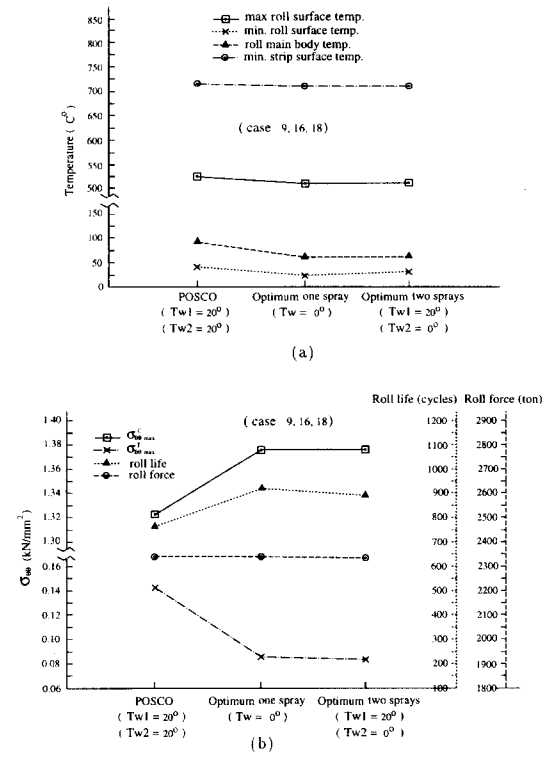
Fig. 12 (a) Roll surface temperature, roll main body temperature and strip surface temperature for various roll cooling practices
(b) $\sigma_{\theta\theta}$, roll force and roll life for various roll cooling practices

Fig. 13 (a) Roll surface temperature, roll main body temperature and strip surface temperature for various roll cooling practices
(b) $\sigma_{\theta\theta}$, roll force and roll life for various roll cooling practices

main body temperature. However, the roll life was extended, since the maximum tensile circumferential stress was decreased, also due to the decrease in the main body temperature, as shown in Fig. 12. Compared to the POSCO design, 13 percent and 10 percent increases in the roll life were noted for the case of one spray zone and for the case of two spray zones, respectively. The present result indicated that there was no definitive advantage of the two spray zones over the one spray zone.

• Optimization of cooling water temperature

In the second trial, optimization was conducted for the determination of both the locations of the spray zones and the cooling water temperature, under the same process conditions and constraints

as given above. The range of the cooling water temperature was taken as $0°C < \mathrm{Tw} < 100°C$. The resulting optimal locations were same as those found in the first trial, for both the one spray zone and two spray zones. For the case of one spray zone, the optimal cooling water temperature was $\mathrm{Tw} = 0°C$. the lowest water temperature possible. Compared to the POSCO design the increase in the roll life was found to be 22 percent, as shown in Fig. 13. Further increase in the roll life compared to the optimal design with $\mathrm{Tw} = 20°C$ was due to the smaller maximum roll surface temperature that led to a greater compressive yield strength. For the case of two spray zones, the optimal cooling water temperatures were such that $\mathrm{Tw}1 = 0°C$ at the delivery side spray zone, and $\mathrm{Tw}2 = 20°C$ at the

entry side spray zone. The resulting increase in the roll life was 18 percent, compared to the POSCO design. When $Tw2 = 0°C$, the resulting maximum roll surface temperature was smaller but the maximum tensile circumferential stress was greater than that obtained when $Tw2 = 20°C$, resulting in a shorter roll life.

2. Concluding Remarks

The effect of various process parameters on the thermo-mechanical behavior of the work roll and on the roll life was investigated, to provide a guideline for the mill designers and shop engineers regarding how to enhance the roll performance. However, the present results address only a part of the roll wear-related problems and there still remain several important developments to be made for roll wear control. They are : 1. for precise evaluation of the effect of the process parameters, explore possible interdependency between the process parameters and if it exists, develop a model to quantitatively correlate them. 2. develop a model for the prediction of the roll life that can reflect the combined effect of both fatigue and abrasion. 3. develop a model for the prediction of the roll wear profile, as it is crucial for the control of the dimensions of the rolled strip. A finite element based model is expected to serve as an effective tool for these developments, as was demonstrated through the present investigation.

Acknowledgements

References

(1) S. Spuzic, K. N. Stranfford, C. Subramanian, and G. Savage: Wear, 1994, Vol. 176, pp. 261~271.
(2) R. V. Williams., and G. M. Boxall: J. Iron steel Inst., 1965, Vol. 203, pp. 369~377.
(3) P. Harper: I&SM, OCTOBER 1988, pp.34~37.
(4) L. F. Coffin: Symp. on Internal Stresses and Fatigue in Metals, Amsterdam, Elsevier, 1959, p. 363.
(5) P. G. Stevens, K. P. Ivens, and P. Harper: J. Iron Steel Inst., 1971, Vol. 209, pp. 1~11.
(6) Y. Sekimoto, K. Tanaka, K. Nakajima, and T. Kawanami: Trans. Iron Steel Inst. Jpn., 1976, Vol. 16, pp.551~560.
(7) J. H. Ryu, O. Kwon, P. J. Lee, and Y. M. Kim: ISIJ International, 1992, Vol. 32, No. 11, pp. 1221~1223.
(8) C. G. Sun, and S. M. Hwang: submitted, 1996.
(9) S. Shida: Journal of the Japan Society for Technology of Plasticity, 1969, Vol. 20, pp. 610~617.
(10) D. M. Parke, and J. L. L. Baker: Iron Steel Eng., 1972, Vol. 49, No. 12, pp. 83~88.
(11) H. G. Baron, and B. S. Bloomfield: JISI, 1961, Vol. 197, p. 223.
(12) K. Sasaki, Y. Sugitani, and M. Kawasaki: J. Iron Steel Inst. Jpn, 1974, vol. 65, pp. 90~96.
(13) J. V. Poplawski, and D. A. Seccombe: Iron Steel Eng., 1980, Vol. 57, pp.47~58.
(14) K. Murata, H. Morise, M. Mitsutsuk, H. Naito, T. Kamatsu, and S. Shida: Trans. Iron Steel Inst., Jpn, 1984, Vol. 24, p. B309
(15) A. Ohnuki, and K. Nakajima: Proc. 4th Int. Conf. on Production Engineering, Tokyo, 1980, pp.1041~1046.
(16) D. E. Goldberg: Genetic Algorithm in Search, Optimization, and Machine Learning, Addison Wesley Publishing Company, 1988.
(17) K. Krishnakumar: SPIE Proceedings, 1989, Vol. 1196, pp. 289~296.
(18) J. S. Chung, and S. M. Hwang: submitted, 1996.